Truck tyre rolling resistance – Experimental testing and constitutive modelling of tyres

Thesis · June 2022

DOI: 10.13140/RG.2.2.24484.39048

1 author:

Jukka Hyttinen
KTH Royal Institute of Technology
13 PUBLICATIONS **74** CITATIONS

KTH ROYAL INSTITUTE
OF TECHNOLOGY

Licentiate Thesis in Vehicle and Maritime Engineering

Truck tyre rolling resistance

Experimental testing and constitutive modelling of tyres

JUKKA HYTTINEN

Stockholm, Sweden 2022

Truck tyre rolling resistance

Experimental testing and constitutive modelling of tyres

JUKKA HYTTINEN

Academic Dissertation which, with due permission of the KTH Royal Institute of Technology, is submitted for public defence for the Degree of Licentiate of Engineering on Wednesday the 15th June 2022, at 9:30 in Sal E3, Osquars backe 14, Stockholm

Licentiate Thesis in Vehicle and Maritime Engineering
KTH Royal Institute of Technology
Stockholm, Sweden 2022

ISBN 978-91-8040-283-5
TRITA-SCI-FOU 2022:31

Printed by: Universitetsservice US-AB, Sweden 2022

Abstract

Global warming sets a high demand to reduce the CO_2 emissions of vehicles. In the European Union heavy-duty road transports account for 6 % of the total greenhouse gases and one of the main factors affecting these emissions is related to the rolling resistance of tyres. The optimal usage of tyres is an important part of solving these challenges, thereby it is important to understand the parameters affecting rolling resistance and the different compromises coupled to them. These compromises could be analysed using computational and experimental methods. To set out the groundwork necessary to minimise the energy consumption of trucks and assess the different parameters affecting tyre behaviour, the following studies have been conducted during this thesis. A framework to model and parametrise truck tyre rubber has been developed for finite element simulations. The presented parallel rheological material model utilises Mooney-Rivlin hyperelasticity, Prony series viscoelasticity, and perfectly plastic networks. A method to reduce tuneable parameters of the model, which significantly simplifies possible parameter studies, is presented. The model has been parametrised using test data from dynamic mechanical analysis of samples from a long haulage heavy truck tyre, and shows a good agreement with the test data. To test the suitability of the modelling technique for tyre simulations, the constitutive model is used in various tyre simulations using the arbitrary Lagrangian-Eulerian method. The material modelling technique is shown to work for static force-deflection as well as dynamic simulations estimating longitudinal force build-up with varying slip levels. Additionally, the modelling technique captures the uneven contact pressure in steady-state rolling, which indicates that the model could also be used in rolling resistance simulations. To study the change of ambient temperature on rolling resistance using experimental methods, a climate wind tunnel is used where the rolling resistance is quantified using a measurement drum. Tests were conducted between -30 °C and +25 °C, and a considerable ambient temperature dependency on rolling resistance was found. Moreover, temperature measurement inside a tyre shoulder is a good indicator for rolling resistance in a broad range of ambient temperatures. Finally, battery-electric long haulage truck driving range calculations are also conducted with varying rolling resistance and air density at different temperatures, showing a significant decrease of driving range with decreasing ambient temperature.

Keywords:
Truck tyre, PRF, filler reinforced rubber, ambient temperature, rubber testing, parametrisation, Finite-element simulation

Sammanfattning

Den globala uppvärmningen ställer höga krav på att minska tunga fordons CO_2-utsläpp. Tunga transporter står för 6 % av de totala växthusgaserna i Europeiska unionen och att fokusera på optimal användning av däck är en viktig del för att minska förorenande växthusgaser. Därför är det viktigt att förstå parametrar som påverkar rullmotståndet och olika kompromisser kopplade till dem. Dessa kompromisser skulle kunna analyseras med hjälp av beräkningsmetoder och experimentella metoder. För att lägga grunden för att minimera energiförbrukningen för lastbilar och bedöma olika parametrar som påverkar däckens beteende, har följande studier genomförts i denna avhandling. Ett ramverk för att modellera och parametrisera lastbilsdäcksgummi utvecklades för finita elementmetod-simuleringar. Den presenterade parallella reologiska materialmodellen använder Mooney-Rivlin hyperelasticitet, Prony-series viskoelasticitet och perfekt plastiska nätverk. En metod har utvecklats för att reducera antalet justerbara materialparametrar i modellen, vilket avsevärt förenklar möjliga parameterstudier. Modellen har parametriserats med hjälp av testdata från dynamisk mekanisk analys och visar en god överensstämmelse mellan testdata och simuleringar. Provstavarna skars ut från ett lastbilsdäck för tunga fordon. För att testa modelleringsteknikens lämplighet användes den konstitutiva modellen i olika däcksimuleringar. Materialmodelleringstekniken har visat sig fungera för statisk vertikalstyvhet såväl som dynamiska simuleringar som uppskattar longitudinell kraftgenerering med varierande slipnivåer och olika friktionskoefficienter. Modelleringstekniken fångar ojämnt kontakttryck vid stationär rullning, vilket indikerar att modellen även kan användas i simuleringar av rullmotstånd. För att studera omgivningstemperaturens inverkan på rullmotståndet med experimentella metoder användes en klimatvindtunnel. Tester utfördes mellan -30 °C och +25 °C och rullmotståndet bestämdes med en mättrumma. Ett avsevärt beroende av omgivningstemperaturen på rullmotståndet påvisades. Dessutom indikerade provningen att temperaturmätning inuti däckskuldran är en bra indikator för rullmotstånd i ett brett område av omgivningstemperaturer. Räckviddsberäkningar för en elektrisk fjärrtransportlastbil utfördes med varierande rullmotstånd och luftdensitet vid olika temperaturer, vilket visade en signifikant minskning av körräckvidden med sjunkande omgivningstemperatur.

Nyckelord:
Lastbildäck, PRF, gummi, förstärkande fyllmedel, effekt av omgivningstemperatur, gummiprovning, parametrisering

Acknowledgements

The project belongs to the Centre for ECO^2 Vehicle Design which is funded by the Swedish Innovation Agency Vinnova (Grant Number 2016-05195). The author is highly grateful to the Centre for ECO^2 Vehicle Design, the strategic research area TRENoP and Scania for their financial support.

I would like to show my gratitude to my kind supervisors Rickard Österlöf, Lars Drugge and Jenny Jerrelind, for their guidance and help during this thesis. In addition, I would like to give special thanks to Matthias Ussner for good teamwork during the climate wind tunnel tests conducted during this thesis.

Södertälje, February 2022
Jukka Hyttinen

Dissertation

This thesis is divided into two parts: Part I gives a brief introduction to the area of research and an overview of the work conducted in this thesis. Part II consists of the following appended papers (**Papers A-C**):

Paper A
J. Hyttinen, R. Österlöf, L. Drugge and J. Jerrelind
Constitutive model suitable for truck tyre rolling resistance simulations.
Proceedings of the Institution of Mechanical Engineers, Part D: Journal of Automobile Engineering (December 2021). DOI: 10.1177/09544070221074108

Hyttinen did the literature survey, wrote the manuscript, designed the test rigs, analysed the test data, developed the parametrisation technique and conducted simulations. Österlöf, Drugge and Jerrelind supervised the work, discussed the research ideas and reviewed the paper.

Paper B
J. Hyttinen, M. Ussner, R. Österlöf, J. Jerrelind and L. Drugge
Effect of ambient and truck tyre temperature on rolling resistance.
Accepted for publication in the International Journal of Automotive Technology (March 2022).

Hyttinen and Ussner performed the tests. Hyttinen did the literature survey, wrote the manuscript, analysed the data and performed the simulations. Ussner, Österlöf, Jerrelind and Drugge reviewed the paper. Österlöf, Jerrelind and Drugge supervised the work and discussed the research ideas.

Paper C
J. Hyttinen, R. Österlöf, J. Jerrelind and L. Drugge
Simulation of a truck tyre using a viscoplastic constitutive rubber model.
Presented at IAVSD2021, 27th Symposium on Dynamics of Vehicles on Roads and Tracks, Aug 17-19, St Petersburg, Russia (2021).

Hyttinen did the literature survey, wrote the manuscript and conducted simulations. Österlöf, Drugge and Jerrelind supervised the work, discussed the research ideas and reviewed the paper.

Publications not included in this thesis

The work carried out during this thesis has also resulted in the following publication:

J. Hyttinen, R. Österlöf, J. Jerrelind and L. Drugge
Development of a vehicle-road interaction analysis framework for truck tyres. Proceedings of the Resource Efficient Vehicles Conference (rev2021), 2021

Table of contents

Part I
OVERVIEW

1 Introduction

A large selling point of heavy-duty trucks is the energy efficiency and total cost of ownership, *i.e.* profitability. Profitability is largely affected by rolling resistance (RR), a commonly known resisting force that resists forward propulsion of the vehicle. This force is generally an unwanted property and plays a key role in optimising truck energy consumption and emissions. Currently, 6 % of the total greenhouse gases in the European Union are produced by the heavy duty transport sector. To reduce these levels, the European Union has set new targets to reduce CO_2 emissions of heavy trucks with 30 % by 2030 compared to a reference vehicle (average certified truck in 2019) [1]. Failure to reach these targets results in significant penalties per manufactured vehicle. This means that the heavy truck segment needs to reduce energy consumption substantially, requiring at least partial electrification of the truck segment. Electric powertrains already have high energy efficiency but the amount of battery capacity in the vehicle is limited. Thereby, RR and aerodynamic resistance account for the largest part of the battery-electric truck (BET) losses, and both are dependent on the surrounding temperature.

Reducing greenhouse gases is essential for economic and ecological purposes, which is why RR is an important parameter to minimise. Tyre manufacturers can affect tyre properties by optimising the tyre structure and rubber compounds whereas truck manufacturers can take into account the optimal usage of tyres in the truck design. Focusing merely on reducing RR might cause unwanted declines in other properties that have conflicting requirements, *e.g.* more rapid wear of tyres and produce of more wear particles, which can be harmful to humans and nature. Hysteresis of rubber is important for braking and handling characteristics, whereas it should be minimised from a rolling resistance perspective. Tyre properties will always be a compromise between different characteristics, which should be balanced according to the requirements of the application.

The purpose of this research is to develop a modelling technique suitable for truck tyre rolling resistance simulations that is easy to parametrise and at the same time captures important rubber properties sufficiently well. This work also aims to provide resourceful information about transient rolling resistance and parameters affecting it, such as the ambient temperature. A visual project description is illustrated in Fig. 1, where both experiments and simulations are important and complement each other. Common finite element rolling resistance simulation models use either hyperelasticity or Prony series. However, the first one cannot simulate viscoelasticity, which causes the majority of rolling resistance [2] and the latter does not capture the strain-amplitude dependency of the storage and loss modulus in rubber. In recent years, nonlinear viscoelastic models have been used in parallel rheological framework to model rolling resistance for passenger car tyres. The drawback of these kind of parallel rheological models is that obtaining material parameters is typically challenging and requires optimisation methods. Additionally, tuning parameters afterwards for sensitivity studies is cumbersome. However, it would be beneficial to have a simple method to obtain material parameters while using an advanced material model that is able to capture important rubber properties for RR simulations.

Tyres are complicated composite products and are affected by different operating conditions. These conditions vary considerably and some of the properties are difficult to simulate. Common test methods neglect the change of ambient temperature, which might lead to false

conclusions if these effects are not taken into account. An example of this is dimensioning batteries for battery-electric trucks; a customer might be dissatisfied with a vehicle if it cannot fulfil the promised driving range at different temperatures. Therefore, it would be useful to test tyres in a wide range of operating conditions to provide better estimates of energy consumption.

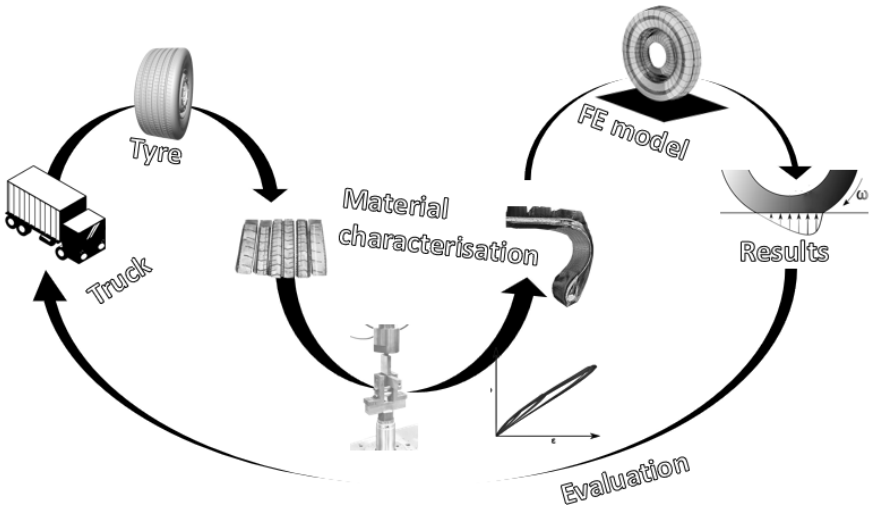

Fig. 1. A visual project description [3].

1.1 Objective

To balance between various performance aspects, the objective has been to develop a rubber modelling and parametrisation framework. This framework should be able to capture dissipation and stiffness properties of filled rubber, which are essential for rolling resistance evaluation as well as for other tyre simulations. To further increase the understanding of different operational conditions affecting rolling resistance, experimental studies should be conducted. The following points should be addressed:

- Developing a suitable finite element modelling technique for tyre rubber
  - A time-domain rubber model that can be used in commercial software
  - Easy tuneability
- Quantifying different operating conditions affecting rolling resistance, *e.g.* effect of ambient temperature on rolling resistance
- Suggesting ways to reduce rolling resistance

The aim is to lay out the groundwork for future finite element rolling resistance simulations and further experimental studies of rolling resistance.

1.2 Thesis outline

The thesis is divided into eleven sections. Section 2 describes the structure of a tyre and the basics of rolling resistance, while Section 3 provides an introduction on important rubber properties. Section 4 introduces testing methods used in this research. The constitutive model used in this thesis is presented in Section 5, and the method to reduce constitutive parameters is established in Section 6. In Section 7, the developed finite element tyre model is presented, and the results from climate wind tunnel tyre rolling resistance tests are given in Section 8. The appended papers are summarised in Section 9 and, finally, conclusions and future work are discussed in Sections 10 and 11, respectively.

2 Tyre basics

Tyres are a fundamental part of trucks, fulfilling many important functions, *e.g.* transmitting longitudinal and lateral forces, absorbing vibrations and carrying load. Pneumatic tyres are suitable for varying axle loads because the inflation pressure can be adjusted accordingly. The composite construction of a tyre consists of many different materials, ranging from polymers, reinforcing fillers, oils, softeners, steels to textiles etc. In this section, a common tyre structure and rolling resistance are discussed briefly.

2.1 Tyre structure

Two types of common tubeless tyres exist, radial and cross-ply tyres, each having different driving characteristics. Radial tyres (Fig. 2 a) are used mainly in truck and passenger car applications while cross-ply tyres (Fig. 2 b) are more commonly used as motorcycle tyres. As the name radial tyre states, these tyres have body cords that go radially from bead to bead (Fig. 3). Additionally, there are two crossing belts close to the contact patch which provide stiffness at the crown area. Cross-ply or diagonal tyres, on the other hand, have two crossing belts going from bead to bead. Cross-ply tyres are cheaper because of the simpler structure but the crossing plies are constantly shearing against each other when the tyre is rolling, creating a larger rolling resistance than radial tyres. In this thesis, the focus is on radial tyres, since they are currently the most commonly used heavy truck tyres.

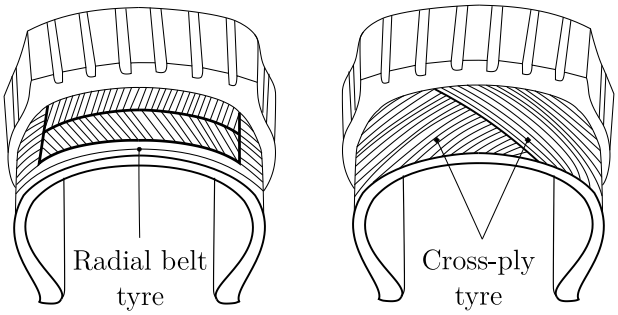

Fig. 2. Belt structure of (a) radial and (b) cross-ply tyre.

Fig. 3 shows a common structure of a radial truck tyre with its most important parts. The structure of a tyre can vary largely but the parts found in almost all radial tyres are tread, sidewall, apex, crown belts, radial belt, bead wire, and inner-liner. The tread is the only part that is usually in contact with the road, transmitting lateral, longitudinal and vertical tyre forces. It is also one of the biggest contributors to rolling resistance [2]. The sidewall provides flexibility and comfort during driving, absorbing vibrations and providing a smooth stiffness gradient from bead to tread [4]. The radial belt or carcass belt is flexible but at the same time, it keeps the air volume of a tyre almost unchanged with different pressure levels. Usually, there are at least two crossing crown belts that keep the crown profile as straight as possible when the tyre has different pressure levels. The crossing crown belts also transmit lateral and

longitudinal forces. The bead wire is a steel wire that keeps the tyre firmly on the rim and provides stability during driving. The inner liner is a thin rubber layer that makes tyres air-tight. It is usually made of a compound containing rubber with low air permeability, such as butyl rubber [5]. Natural and synthetic rubber are not suitable as an inner liner since they cannot keep high pressurised air inside the tyre for an extended period of time.

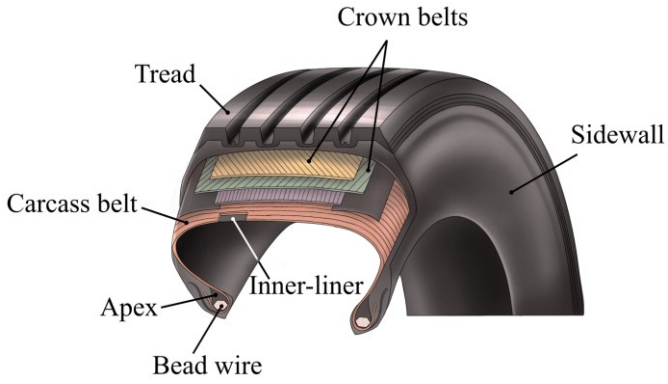

Fig. 3. A structure of a radial truck tyre showing the most common parts.

2.2 Tyre rolling resistance

Rolling resistance is a force that resists vehicle motion. It has been a prioritised property since the oil crisis of the 1970s. Recently, there has been a renewed interest in rolling resistance partly because of global warming but also because of the transition to battery-electric trucks. The body of literature accepts that rolling resistance is largely (80-95 %) caused by viscoelasticity in rubber [6]. Because of this viscoelasticity, the peak of the contact pressure of a tyre is shifted in front of the tyre rotation axis in rolling motion (Fig. 4). This causes a braking moment opposing the vehicle motion. The remaining factors of rolling resistance are caused by effects such as friction and aerodynamic resistance [2].

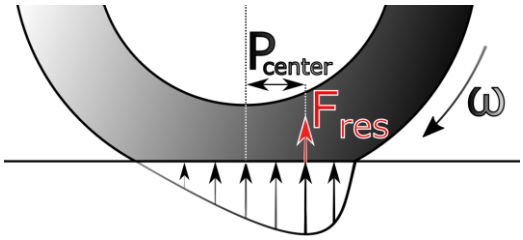

Fig. 4. Tyre contact pressure in a rolling motion, which creates a braking moment that resists vehicle motion [3].

A widely accepted definition of rolling resistance is the energy consumed by a unit distance $\left[\frac{J}{m}\right]$. In this thesis, a rolling resistance definition introduced by Schuring [7] is used. This definition assumes a full conversion of mechanical energy into heat as stated in Eq. (1).

$$F_r = \frac{P_r}{v} = \frac{P_{in} - P_{out}}{v}, \tag{1}$$

where P_r is the rolling resistance power, P_{in} is the input power for the tyre, P_{out} is the measured output power, and v is the vehicle speed. This definition allows the rolling resistance to be measured using different testing methods, *e.g.* force, torque, power and deceleration method. Rolling resistance is often described as a rolling resistance coefficient (C_{rr}), which essentially describes the ratio between longitudinal (F_r) and vertical force (F_z). This ratio is often multiplied by a thousand to make C_{rr} easier to read (Eq. (2)). In this case, the unit is kg/ton.

$$C_{rr} = 1000\frac{F_r}{F_z}. \tag{2}$$

3 Rubber properties

In this section, a summary of important rubber characteristics is provided as a background. Rubber is a polymer and has many interesting properties such as nonlinear elasticity [8] and strain softening [9]. The name polymer comes from the Greek language and the words “polus” and “meros” mean “many parts”. The name describes the essential structure of polymers, which have numerous repeated long chain units. Tyre rubber consists of different polymers combined with reinforcing fillers. These fillers add many particular properties to rubber, *e.g.* strain amplitude-dependent stiffness (storage modulus) and damping (loss modulus) commonly referred as the Fletcher-Gent effect or Payne effect, more pronounced strain-softening known as the Mullins effect and viscoelasticity. Filled rubber is at the same time flexible, wear-resistant and provides excellent adhesion between many surfaces.

3.1 Nonlinear elasticity

Nonlinear elasticity originates from the change in entropy (polymer chain straightening), unlike metals, which have energetic elasticity (change of distance between the atoms) [10]. Because of the straightening of the polymer chains, the volume is almost unchanged during deformation if the rubber is not exposed to large pressure loads to all outer surfaces. Even though polymers deform almost without volume changes in shear and tension, they have substantially lower bulk modulus than metals.

3.2 Viscoelasticity

Materials having both elastic and viscous properties are called viscoelastic materials. In the rubber structure, viscoelasticity can be related to the entangled polymer chains, which straighten when the rubber is stretched. Due to entanglements, the straightening does not occur immediately. Thereby, with sudden displacement, the stresses start to relax over time reaching elastic (long term) stress after viscous stresses are fully relaxed.

3.3 Mullins effect

Strain softening in rubber is often referred to as the Mullins effect. This essentially means that the properties keep changing with the previously applied maximum strain level [9]. During mechanical analysis, samples should be preconditioned with realistic strain levels so that rubber properties do not change during the tests if the intention is not to model the Mullins effect. Also, it is important to take this effect into account when preconditioning new tyres with realistic axle loads, to avoid measuring the break-in of the tyres instead of measuring the actual rolling resistance. The Mullins effect is also present in unfilled rubber but the effect is stronger in filler reinforced rubber. The Mullins effect can be reversed with temperature conditioning [9].

3.4 Fletcher-Gent effect

The addition of reinforcing fillers to a rubber adds a strain amplitude dependency for storage modulus, often called the Fletcher-Gent effect. Both the Fletcher-Gent and Mullins effect

have similar qualities and are sometimes difficult to separate from each other. The main differentiating factor between them is that the Fletcher-Gent effect is present regardless of previously occurred strain amplitudes and is a reversible effect. The Mullins effect, on the other hand, is not reversible in normal conditions [9]. The Fletcher-Gent effect is sometimes explained as a breakage of the bonds between the filler and polymer chains [11]. Modelling of this effect is important when the strain range in the application changes at different parts.

3.5 Glass transition temperature

Polymers have a glass transition temperature (T_g) that describes the transition from a rubber-like material (viscoelastic), to a brittle glass-like material [8]. In a tyre application, the glass transition temperature is used as a parameter to tune the trade-off between grip and RR [5]. Generally, a lower glass transition temperature equates to a smaller rolling resistance and lower heat build-up, whereas in the opposite case the wet grip is increased [5]. For vulcanised natural rubber, the glass transition temperature is roughly at -68 °C and for vulcanised synthetic rubber -55 °C [12]. Tyres are always designed to have a considerably lower T_g than their usage temperature range to maintain flexibility, comfort and good wear properties.

4 Experimental methods

The experimental methods used in this thesis are dynamic mechanical analysis (DMA), thermogravimetric analysis and international rubber hardness (IRHD) measurements for tyre rubber. Additionally, tyre temperature and rolling resistance measurements were conducted in a climate wind tunnel. A summary of these testing methods is described in this section.

4.1 Dynamic mechanical analysis

DMA is used to measure the mechanical properties of rubber (stress-strain) and the results are used to parametrise the simulation models. Two deformation modes are studied in this thesis: uniaxial tension and simple shear. The test samples were extracted from a tyre section. A custom-made double shear test rig, as shown in Fig. 5, was used for tyre rubber measurements.

*Fig. 5. Double shear testing rig for tyre rubber (**Paper A**).*

For an incompressible material, the deformation gradient for the uniaxial case becomes [8]:

$$\boldsymbol{F}_{uniaxial} = diag\left[\lambda(t), \lambda(t)^{-\frac{1}{2}}, \lambda(t)^{-\frac{1}{2}}\right], \tag{3}$$

and for simple shear:

$$\boldsymbol{F}_{simple\ shear} = \mathbf{I} + \gamma(t)\boldsymbol{e}_1 \otimes \boldsymbol{e}_2, \tag{4}$$

where $\mathbf{I}$ is the identity tensor, λ is the stretch ratio, and γ is the shear strain. From DMA, two different scalar values, storage and loss modulus, are extracted. The storage modulus describes the stiffness of a material, which is calculated as a secant modulus from the tests data

(Fig. 6). Shear (G') and tensional (E') storage modulus are calculated from the maximum stress and strain values:

$$G' = \frac{\tau_{amp}}{\gamma_{amp}}, \quad E' = \frac{\sigma_{amp}}{\varepsilon_{amp}}, \tag{5}$$

where τ_{amp} and σ_{amp} are the shear and tensional stress amplitude, and γ_{amp} and ε_{amp} are the shear and tensional strain amplitude.

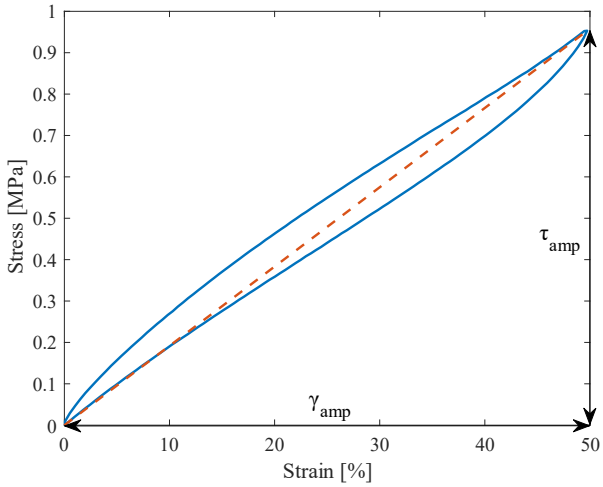

*Fig. 6. Storage modulus is a secant modulus (red) calculated from the maximum stress (τ_{amp}) and strain (γ_{amp}) levels from a hysteresis loop (blue) (**Paper A**).*

Shear (G'') or tensional (E'') loss modulus can be calculated from the equivalent loss angle $tan(\delta_{eqv})$ and storage modulus (G' or E'):

$$G'' = G' tan(\delta_{eqv}), \quad E'' = E' tan(\delta_{eqv}). \tag{6}$$

The loss angle (Eq. (7)) is calculated from the dissipated energy (W) and stress (τ_{amp}) and strain amplitudes (γ_{amp}).

$$tan(\delta_{eqv}) = \frac{W}{\pi \tau_{amp} \gamma_{amp}}. \tag{7}$$

The dissipated energy is calculated in the following way for one hysteresis loop [13]:

$$W = \oint \tau \, d\gamma = \int \tau \dot{\gamma} dt. \tag{8}$$

4.2 Thermogravimetric analysis

Thermogravimetric analysis (TGA) can be used to reverse engineer different compositions in a polymer [5]. In this work, the amount of carbon black reinforcing filler in different tyre rubber samples was of interest because carbon black affects both the stiffness and hysteresis of rubber. In TGA, rubber pieces are kept in a chamber where the temperature is increased stepwise. Throughout the measurement, the mass of the test specimen is observed. By knowing the temperature at which different materials deteriorate, the weight percentage of different compounding material can be reverse engineered (Fig. 7). More information regarding TGA can be found in SS-ISO 9924-3:2009 [14].

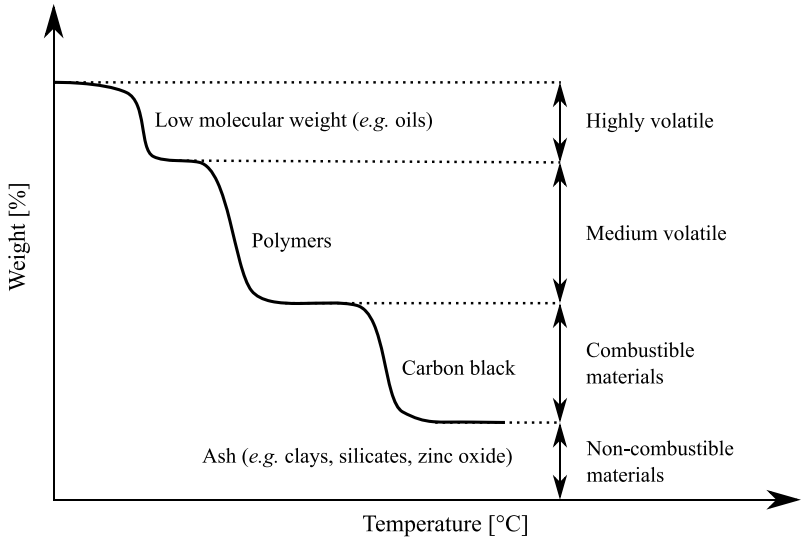

Fig. 7. The measurement principle in TGA.

4.3 Hardness measurements

Hardness is an important measure since it correlates with the amount of rubber fillers (*e.g.* carbon black), thereby also stiffness and dissipation qualities [15]. International rubber hardness degrees micro (IRHD M) is a scale used to indicate the hardness of elastomeric materials. Another common hardness scale used for rubbers is Shore hardness. Further information on the IRHD M testing method can be found in SS-ISO 48-2:2018 test standard [16].

4.4 Climate wind tunnel rolling resistance testing

Very little information exists on how rolling resistance is affected by cold ambient temperatures. Thereby, a climate wind tunnel was utilised to regulate wind and ambient temperature during rolling resistance testing. The used climate wind tunnel is discussed in detail by Duell *et al.* [17].

The tyre rolling resistance force (F_r) is directly measured in the climate wind tunnel. Often in RR measurements, parasitic losses $\left(F_p\right)$ are subtracted from the tyre measurements as can be seen from Eq. (9). In this thesis, parasitic losses are defined as losses originating from the measurement device itself. F_p is a drum measurement, taken after rotating the drum for 30 minutes without the truck on the measurement drum.

$$C_{rr}(\mathrm{t}) = 1000\frac{F_r(t) - F_p}{F_z}. \tag{9}$$

Wheel bearing losses and aerodynamic losses from the rotating tyre are considered to be part of the rolling resistance in the tests conducted during this research. The widely used testing standard ISO 28580:2009 [18] defines parasitic losses slightly differently and does not include bearing or aerodynamic losses to the tyre measurements. When using a truck drive axle in the measurements, the axle load cannot easily be controlled accurately enough to use the ISO 28580 parasitic loss definition.

The tyre temperature was measured during the tests using thermocouples that were drilled inside the tyre and glued using Loctite 3090 glue. Two separate places, the tyre shoulder and tyre apex (Fig. 8 a), were chosen. Additionally, one test was conducted where water was sprayed on the tyre to quantify its cooling effect on rolling resistance (Fig. 8 b).

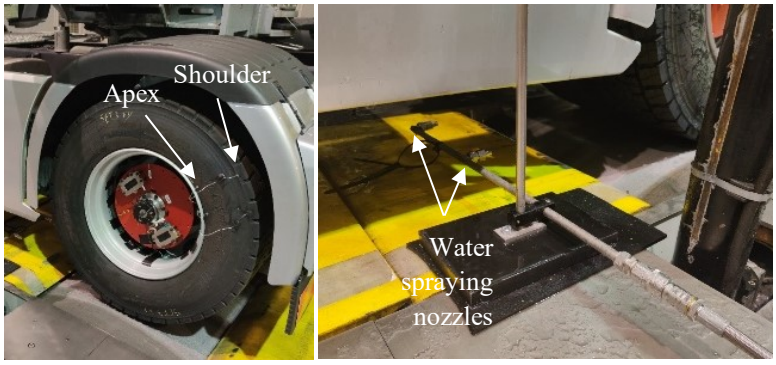

*Fig. 8. (left) Rolling measurement setup with temperature sensors and measurement drum. (right) Water spraying nozzles in front of the tyre (**Paper B**).*

Fig. 9 shows the measurement truck in the test cell at -30 °C temperature. It can be seen that the surroundings of the truck are near -30 °C, whereas the tyre temperature is considerably higher than 0 °C. This is already a significant indicator that rolling resistance is high, since a large amount of rubber has been warmed to a substantially higher temperature than the surroundings.

*Fig. 9. Heat camera picture of the truck in the climate wind tunnel at -30 °C. The tyres on the roller have a considerably higher temperature than the surrounding temperature (**Paper B**).*

Drum measurements are approximations of real-road conditions and produce a different kind of contact pressure than a flat road. Multiple correction equations exist, of which Clark's equation [19] is one of the most widely used to adjust drum rolling resistance coefficients (C_{rr_drum}) to flat road values $(C_{rr\_flatroad})$:

$$C_{rr\_flatroad} = \frac{C_{rr\_drum}}{\sqrt{1 + \frac{r_{tyre}}{r_{drum}}}}, \tag{10}$$

where r_{tyre} and r_{drum} are the tyre and drum radius. The measurements shown in this thesis are not corrected to flat road values.

5 Constitutive rubber model

A short background of different rubber modelling techniques is introduced and discussed here. There have been some studies regarding truck tyre simulations, but the largest part of the work regarding rolling resistance analyses is focused on the passenger car segment. In truck tyre rolling resistance simulations, hyperelastic models have been utilised by Rodkwan and Daesa [20] and Ali *et al.* [21]. However, hyperelastic models cannot model viscoelasticity, which causes the major part of rolling resistance [2]. Thereby, more advanced models should be utilised. The most widely used linear viscoelastic model in tyre simulations is Prony series [22], [23]. Prony series is used in combination with some kind of hyperelastic model, such as the Neo-Hookean or the Mooney-Rivlin model. The limitation with these linear viscoelastic models is that they are not able to represent the amplitude dependency for the storage and loss modulus of rubber.

To model stiffness and dissipation of the rubber material at the same time, there exist three different popular methods: viscoplasticity [24]; nonlinear viscoelastic models [25]; and fractional derivatives [26]. Previously, Rafei *et al.* [25] utilised the Bergström-Boyce (BB) material model in a parallel rheological framework (PRF). The Bergström-Boyce model is a large improvement over the Prony series. However, these models are difficult to parametrise; some parameters become unclear when BB is used in a PRF, and parameter tuning for sensitivity studies is problematic. Additionally, some nonlinear viscoelastic models (*e.g.* Bergström-Boyce, Power law strain hardening or Hyperbolic-sine model) might require extremely small ($< 10^{-27}$) parameters in some unit systems, which might cause numerical instabilities [27]. In bushing simulations, fractional derivatives and hyperviscoplastic models have become popular. Most of the commercial implementations of fractional derivative models are in the frequency domain only. In this thesis, a hyperviscoplastic parallel rheological framework is used, which has separate hyperelastic, viscous and hyperelastoplastic parts (Fig. 10). All the finite element simulations were conducted using the commercial finite element software MSC Marc. Previously, Austrell and Olsson have successfully used a similar modelling technique for industrial rollers [28]. The advantage of this modelling method is that the contributions can be tuned separately, which is beneficial for sensitivity studies.

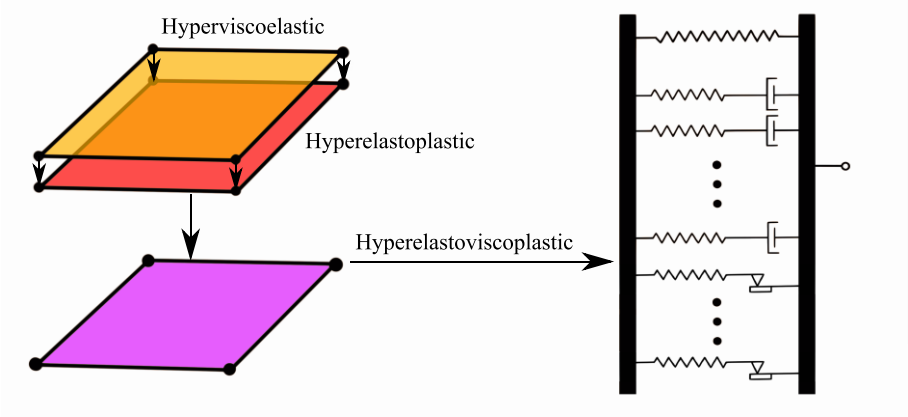

*Fig. 10. Parallel scheme of the hyperelastoviscoplastic material model (**Paper A**).*

Different hyperelastic, viscoelastic and plastic networks are organised in parallel, which is why the total stress is the sum of the hyperelastic model $(\boldsymbol{\sigma}_{hyperelastic})$, viscous stresses $(\boldsymbol{\sigma}_{viscous,i})$ and hyperelastoplastic stresses $(\boldsymbol{\sigma}_{hyperelastoplastic,j})$ according to Eq. (11).

$$\boldsymbol{\sigma}_{tot} = \boldsymbol{\sigma}_{hyperelastic} + \sum_{i=1}^{V} \boldsymbol{\sigma}_{viscous,i} + \sum_{j=1}^{P} \boldsymbol{\sigma}_{hyperelastoplastic,j}. \tag{11}$$

5.1 Hyperelasticity

Rubber elasticity is nonlinear and generally has 10^4 larger bulk modulus than shear modulus [13]. In other words, most of the stresses come from the shape-changing properties, because the bulk modulus is many orders of magnitude larger than the shear modulus. Hyperelastic models describe the reversible nonlinear elastic behaviour of rubber. These kinds of models are an important part of the PRF model since fully viscous models cannot hold load after the material has relaxed. There are two types of hyperelastic models: mechanistic and phenomenological models. Mechanistic models, such as Neo-Hookean [8] or Arruda-Boyce [29], describe the internal structure of rubber, whereas phenomenological models depict an empirical relationship between stress and strain. Examples of phenomenological models are Mooney-Rivlin [30] and Ogden [8].
For nearly incompressible framework, the strain energy density function (W_{tot}) is often divided into volumetric (W_{vol}) and deviatoric (W_{dev}) parts:

$$W_{tot} = W_{vol} + W_{dev}. \tag{12}$$

MSC Marc uses Eq. (13) as its volumetric strain energy density function.

$$W_{vol} = \frac{9}{2}\kappa\left(J^{1/3} - 1\right)^2, \tag{13}$$

where κ is the bulk modulus and J (volume ratio) is the determinant of the deformation gradient (F). For Mooney-Rivlin, MSC Marc 2021 approximates automatically from the parameters $\kappa = 10\ 000(c_{10} + c_{01})$. Poisson's ratio (ν) describes the relation between transversal and axial strain in deformation. With nearly incompressible modelling approach, the Poisson's ratio is slightly below 0.5 to avoid numerical instabilities [31].

Most hyperelastic models characterise the stress-strain behaviour with the help of deviatoric strain invariants ($\bar{I}_1$ and/or $\bar{I}_2$, Eq. (14)). These invariants are calculated using eigenvalues $(\lambda_1 - \lambda_3)$ of the modified right Cauchy-Green tensor $(\bar{\boldsymbol{C}})$:

$$\begin{aligned} \bar{I}_1 &= {\lambda_1}^2 + {\lambda_2}^2 + {\lambda_3}^2 \text{ and} \\ \bar{I}_2 &= {\lambda_1}^2{\lambda_2}^2 + {\lambda_1}^2{\lambda_3}^2 + {\lambda_2}^2{\lambda_3}^2. \end{aligned} \tag{14}$$

The models utilising only the first invariant (*e.g.* Yeoh) do not benefit greatly from having test data from additional deformation modes compared to models utilising two different strain invariants. On the other hand, models using the second invariant might have more control

over the ratio between uni- and biaxial deformations. There are also models that utilise deviatoric principal stretches, *e.g.* Ogden [8].

The base stiffness of the PRF model described in **Papers A** and **C** is the Mooney-Rivlin (Eq. (15)), which has two constitutive parameters, c_{10} and c_{01}. The strain energy density function $\left(W_{Mooney-Rivlin}\right)$ of the Mooney-Rivlin is the following:

$$W_{Mooney-Rivlin} = c_{10}(\bar{I}_1 - 3) + c_{01}(\bar{I}_2 - 3). \tag{15}$$

5.2 Prony series

Linear viscoelastic models are the most commonly utilised methods to simulate viscoelasticity in rubber. Despite the name linear viscoelastic, they have a nonlinear stress response (Fig. 12 a) while the viscous flow is linear, *e.g.* viscous stresses are proportional to the strain rate. For filled rubber used in tyres, the Prony series is insufficient, since the storage and loss modulus in shear produced by the Prony series is constant for different strain amplitudes. This linearity over different strain amplitudes is highlighted in Fig. 11. Some models, such as Yeoh, might produce non-constant storage and loss modulus over strain amplitudes but this amplitude dependency is not built into the Prony series itself.

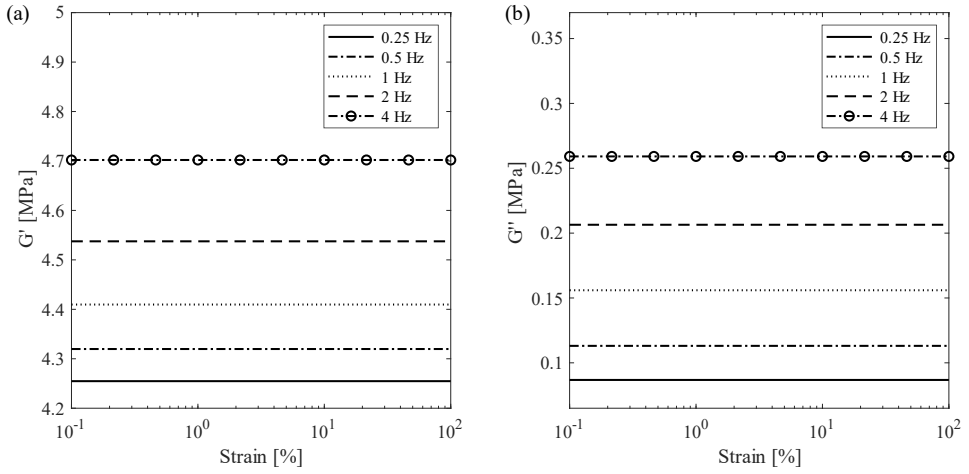

Fig. 11. Prony series produces constant (a) storage (G') *and (b) loss* (G'') *modulus curves in simple shear, depending on the chosen hyperelastic model (**Paper C**).*

In this work, the Prony series is used in combination with Mooney-Rivlin. The total viscoelastic model can be written in terms of a time-dependent stress relaxation function $\left(G_r(t)\right)$. G_0 is the hyperelastic stress-strain function, whereas the term- $\sum_{i=1}^{V} g_i \left(1 - e^{-t/\tau_i}\right)$ describes the viscous stress relaxation. τ_i is the i^{th} relaxation time for the viscous networks (Eq. (16)).

$$G_r(t) = G_0\left(1 - \sum_{i=1}^{V} g_i\left(1 - e^{-t/\tau_i}\right)\right). \quad (16)$$

Normalised storage (g') modulus can be written in the frequency domain in the following way:

$$g'(\omega) = \left(1 - \sum_{i=1}^{V} g_i\right) + \sum_{i=1}^{V} \frac{\tau_i^2 \omega^2 g_i}{\tau_i^2 \omega^2 + 1}, \quad (17)$$

where ω is the angular frequency and V is the number of viscoelastic networks. Similarly, normalised loss modulus (g'') can be written as:

$$g''(\omega) = \sum_{i=1}^{V} \frac{\omega \tau_i g_i}{\tau_i^2 \omega^2 + 1}. \quad (18)$$

5.3 Plasticity

The chosen plastic model utilises the Ogden [8] hyperelastic model with perfect plasticity. The hyperelastic model is expressed as:

$$W_{Ogden} = \sum_{i=1}^{N} \frac{\mu_i}{\alpha_i}\left(\bar{\lambda}_1^{\alpha_i} + \bar{\lambda}_2^{\alpha_i} + \bar{\lambda}_3^{\alpha_i} - 3\right), \quad (19)$$

where $\bar{\lambda}_k^{\alpha_i} = J^{-\frac{\alpha_i}{3}} \lambda_k^{\alpha_i}$ are the deviatoric stretch ratios and N is the amount of Ogden terms. This model has two parameters per Ogden term, (I) α_i and (II) μ_i. A perfectly plastic model has an additional parameter for yield stress. These plastic models can be stacked in parallel to produce different stress-strain shapes. The Ogden model can be set to behave identically to the Mooney-Rivlin, with the parameters $\mu_1 = 2c_{10}$, $\mu_2 = -2c_{01} = -2\frac{c_{10}}{7}$, $\alpha_1 = 2$ and $\alpha_2 = -2$.

5.4 Parallel rheological model

The previously described hyperelastic, viscous and plastic networks are organised in parallel in the PRF model. The hysteresis loops from the viscoelastic (Fig. 12 a) and plastic (Fig. 12 b) models are added together to create the total response (Fig. 12 c) of the model.

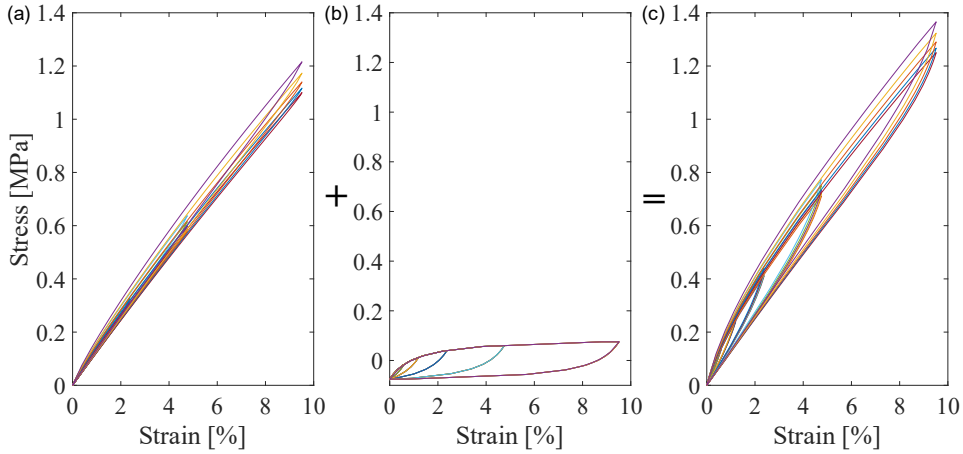

Fig. 12. (a) Viscoelastic and (b) plastic stresses generate (c) the total stress response in the PRF model [3].

The viscoelastic networks create the frequency dependency, and the plastic networks provide the amplitude dependency. These contributions are showcased in Fig. 13, where the Prony has a frequency dependency and virtually zero strain amplitude dependency in shear. The plastic models create the strain amplitude dependency without adding any additional frequency stiffening. This kind of constitutive model can capture amplitude and frequency dependency trends of the storage and loss modulus, as can be seen in Fig. 14, where tests and simulation data are presented next to each other with good agreement. Because of the parallel scheme, the frequency dependency is unchanged throughout the frequency range, which is a slight drawback but at the same time makes parametrisation simpler. Nevertheless, this approach is a sufficient approximation of the Fletcher-Gent effect if the strain range is not too wide (Fig. 14).

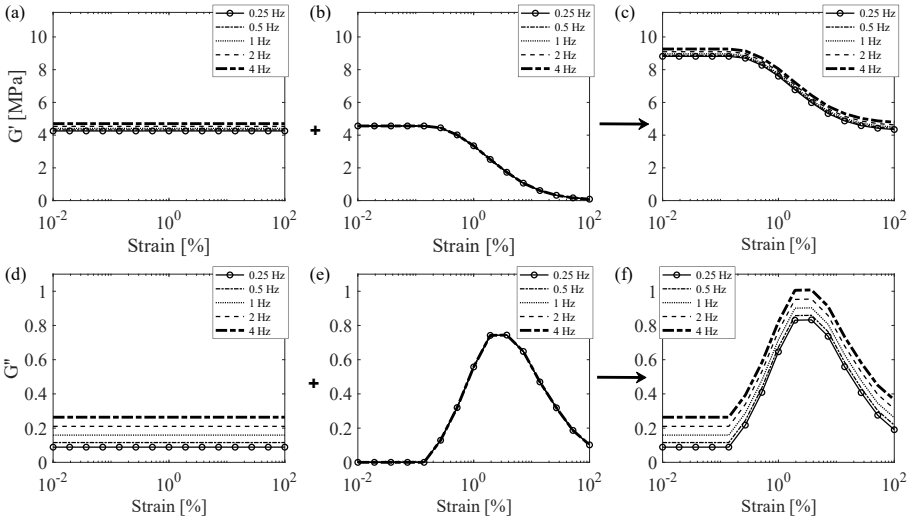

*Fig. 13. Illustration of different contributions to the total response of the material model. (a) and (d) show the storage and loss modulus produced by the Prony series; (b) and (e) depict storage and loss modulus from the plastic networks; and (c) and (f) show storage and loss modulus plots from the whole material model (**Paper C**).*

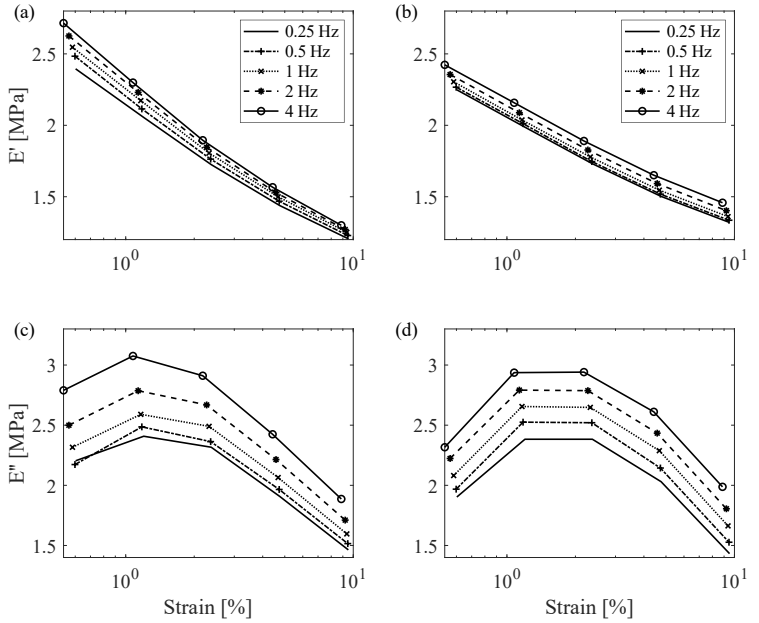

*Fig. 14. Tested (left) and simulated (right) rubber sample in tension, storage (a, b) and loss (c, d) modulus (**Paper C**).*

6 Parameter reduction

Generally, obtaining constitutive parameters is difficult. The previously introduced PRF model has a large number ($N = 2 + 2V + 5P$) of parameters which makes it difficult to obtain those parameters depending on the amount of viscoelastic (V) and plastic (P) networks. A method is shown here to reduce these material parameters to six. These reduced parameters are beneficial in modelling since the number of tuneable parameters does not increase, even if additional viscoelastic or plastic networks are added. **Paper A** shows that through this method the material model can be parametrised, even using manual iterations. **Paper A** utilised 40 Prony elements and eight plastic networks, where the total amount of independent parameters is 122. It is necessary that the model is implemented in some software package (*e.g.* MATLAB or Python), since simulating the model in finite element software is time-consuming even using only one element.

6.1 Hyperviscoelastic model

The Mooney-Rivlin parameters are set to be dependent on each other with $\frac{c_{10}}{c_{01}} = 7$. This type of approach has been used previously by Anand *et al.* [32]. This ratio means that the contribution from uni- and biaxial strains to stresses is fixed, thereby only one parameter needs to be tuned.

Österlöf *et al.* [33] reduced the parameters by setting the stiffening parameters equal for all the viscoelastic networks and distributing all the time coefficients linearly over logarithmic space. This is a good method, but produces only a narrow range of increasing loss modulus. This research utilises a similar approach except that the time coefficients are distributed over logarithmic space using the power function:

$$\tau_i(y_i) = 10^{l-\left((i-1)\frac{1}{V-1}\right)^{0.5}(l-u)}, i = 1 \dots V, \tag{20}$$

where V is the number of viscoelastic networks, l is the lower and u is the upper limit for distributing the time coefficients. The frequency range is set with the parameters l and u. The amount of viscoelastic networks needed depends on the required frequency range. The wider the range, the more viscoelastic networks are needed, as illustrated in Fig. 15. This figure shows storage and loss modulus plots in a wide frequency range using different amounts of viscoelastic networks. By using too small a number of networks, the plots have unphysical peaks. The effect of parameter l is depicted in Fig. 15 (c) and (d).

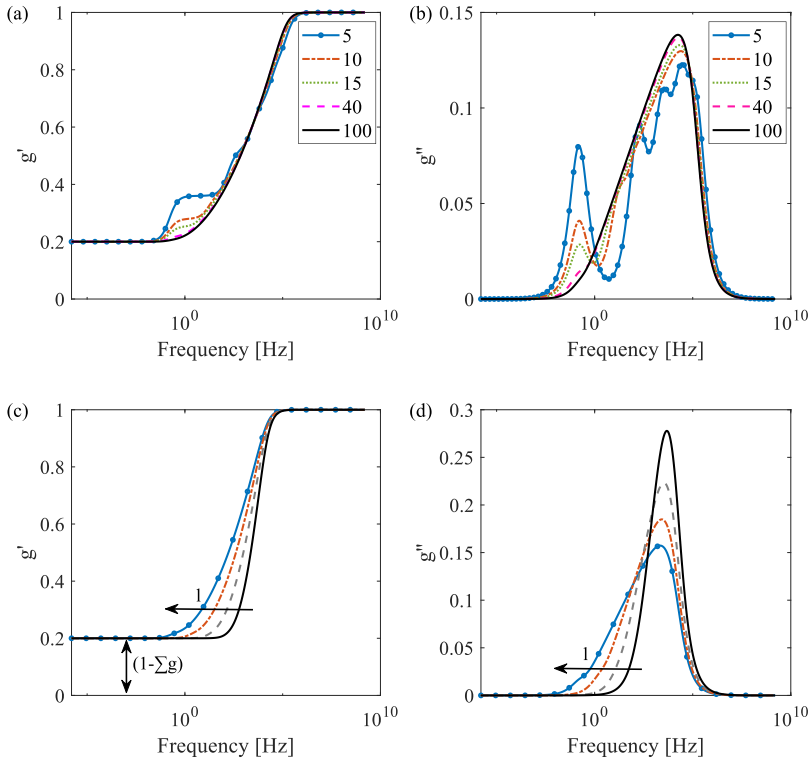

Fig. 15. If the required frequency range is wide, a larger number of Prony networks is needed so that storage (a) and loss modulus (b) plots do not produce unphysical peaks in storage and loss modulus curves. The variation of parameter l is shown in figures (c) and (d). $(1 - \sum g)$ *is the elastic response at low frequencies (**Paper A**).*

6.2 Elastoplastic model

The Ogden model is used merely because the Mooney-Rivlin model is not available in the PRF model in MSC Marc 2021. However, the Ogden model can be set to behave equally as the Mooney-Rivlin by choosing the parameters according to Eq. (21) for different plastic networks.

$$\begin{aligned} \mu_{1n} &= 2c_{10n}, \qquad \mu_{2n} = -2c_{01n} = -2\frac{c_{10n}}{7}, \\ \alpha_{1n} &= 2, \qquad \alpha_{2n} = -2, \qquad n = 1..P, \end{aligned} \tag{21}$$

where P is the number of plastic networks. The shear modulus μ_{1n} is then set to decrease linearly from network to network. Yield stress is set to increase linearly. The shear modulus is distributed with the parameter h, and yield stresses with the parameter s. By fixing the ratio between these parameters, $r = \frac{h}{s}$, h can be used to adjust the slope of storage and loss

modulus curves, while r describes the horizontal shift of the storage and loss modulus curves caused by the plastic networks (Eq. (22)). Fig. 16 shows hysteresis curves produced by different networks using this method and the summed response from all of the plastic networks. The effects of different reduced plastic parameters r and h on storage and loss modulus curves are highlighted in Fig. 17 a-d.

$$\mu_{1n} = (P - n + 1)h, \qquad \mu_{2n} = \frac{\mu_{1n}}{7},$$
$$S_n = ns = n\frac{h}{r}, n = 1..P. \tag{22}$$

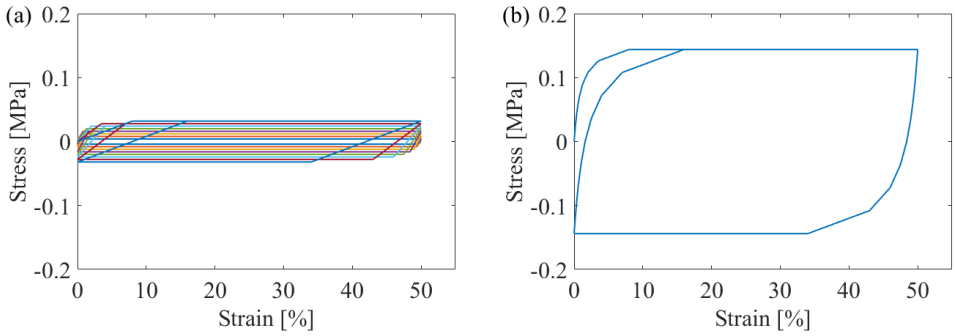

Fig. 16. (a) Perfectly plastic networks separately and (b) response from all the parallel plastic networks.

Using this parameter reduction technique, the simulations result in a physical-like behaviour, even above the frequency range of the test data, if the parameter u is set to be small enough, *i.e.* the limit of the highest required frequency is large enough. Because the time coefficients are fixed into the chosen distribution function, the storage and loss modulus increase almost linearly over a logarithmic x-scale in a wide range of frequencies, which is typical behaviour for filler reinforced rubber. Surface plots of storage and loss modulus in a wide frequency and strain amplitude range are shown in Fig. 18 (a) and (b). For more information regarding the influence of remaining parameters on storage and loss modulus curves, see **Paper A**.

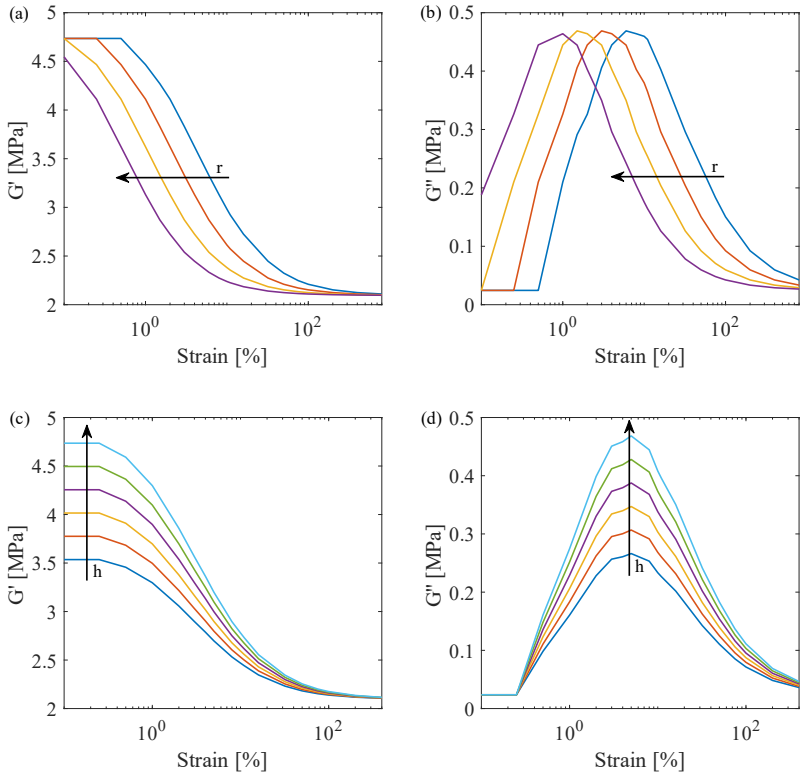

*Fig. 17. Parameter variation of r and h when there is no viscoelasticity; (a) and (c) show the effect of h and r on storage modulus, while (b) and (d) show the effect on loss modulus (**Paper A**).*

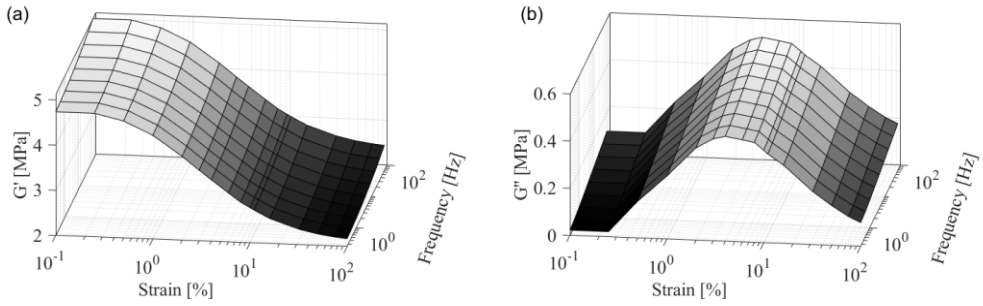

Fig. 18. Amplitude and frequency dependency for the parametrised material model; (a) Storage modulus G' and (b) loss modulus G''.

7 Finite element tyre model

The tyre model used in **Paper C** is introduced in the following paragraphs. The model was created to initially evaluate the suitability of the hyperviscoplastic constitutive model for different tyre simulations. The arbitrary Lagrangian-Eulerian (ALE) method was used in these simulations. This method has two advantages over the pure Lagrangian method: (I) simulations can be started from steady state, and (II) the used mesh does not need to be equispaced (Fig. 19). The simulations use the previously deformed mesh to rotate material through the mesh, which significantly reduces the computational effort. The road has been modelled as a rigid surface. Simulations start by inflating the tyre to the desired inflation pressure. After this, the road is pressed against the tyre, simulating different axial forces.

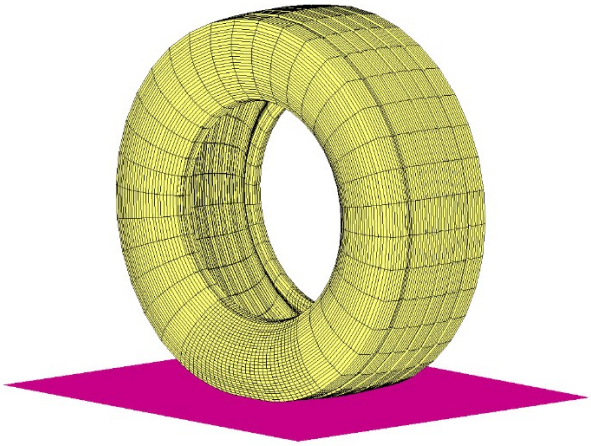

*Fig. 19. Finite element model of the tyre using non-equispaced mesh (**Paper C**).*

Fig. 20 shows the vertical stiffness of the tyre when different pressure levels were used. With increasing tyre inflation pressure, the tyre becomes stiffer. Another effort to test this modelling technique was to vary the slip ratio in rolling to see the suitability of the model for the longitudinal force generation. Fig. 21 depicts the longitudinal force produced with two different friction coefficients and varying slip ratios.

Viscoelasticity causes the largest part of rolling resistance [2]. Therefore, to simulate the rolling resistance of a tyre, the model should be able to simulate viscoelasticity with sufficient accuracy. This viscoelasticity creates an uneven contact pressure in rolling, which should be captured in the simulation framework. Because of the uneven contact pressure, the centre of pressure created by the contact surface shifts in front of the tyre rotation axis. This centre of pressure then creates the rolling resistance braking moment (Fig. 4). In steady state rolling, the finite element tyre model seems to capture this uneven contact pressure (Fig. 22).

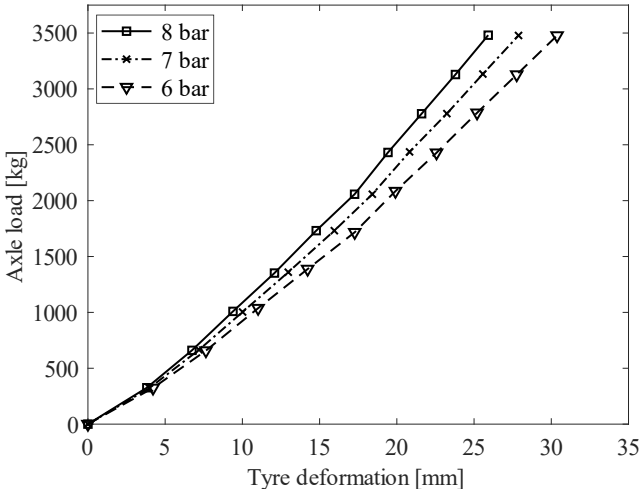

*Fig. 20. Vertical stiffness of the tyre using different inflation pressure levels (**Paper C**).*

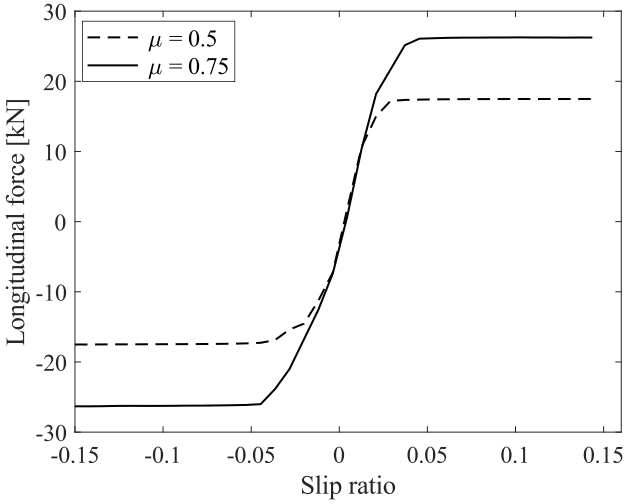

*Fig. 21. Longitudinal force generation of the model using two different friction coefficients (**Paper C**).*

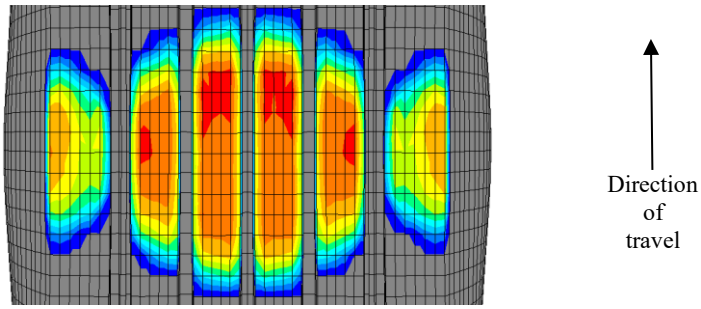

*Fig. 22. The uneven contact pressure of the tyre in steady-state rolling (**Paper C**).*

8 Temperature effect on rolling resistance

It is commonly known that temperature has a significant effect on rubber stiffness as well as hysteresis, *i.e.* energy dissipation; therefore, it will also affect rolling resistance. However, only a handful of studies exist that analyse the effect of ambient temperature [34], [35] on rolling resistance or transient rolling resistance [36]–[39]. Ejsmont *et al.* [34] have studied the effect of ambient temperature on a truck tyre in a range between +4 to +38 °C. They concluded that during the rolling resistance measurements the tyre temperature should be observed, and the test should always be conducted at the same temperature to acquire comparable results. They did not include the effect of wind in their measurements. Ejsmont *et al.* [40] have also studied the effect of road wetness on passenger car tyres, reporting a significant increase in rolling resistance in wet conditions. They noted that part of the increase in rolling resistance in these tests could be because of pumping water away from the contact patch, and the whole increase could not be explained by the decrease of tyre temperature. The vast majority of rolling resistance tests are conducted at +25 °C and the results are represented as a constant stabilised value, neglecting the transient rolling resistance. Sandberg *et al.* [41] have previously studied transient effects of temperature on truck tyre rolling resistance with varying velocity. They created a simulation model that approximates tyre temperature when stabilised rolling resistance is known at different velocity levels.

In this thesis, the rolling resistance of a 315/70 R22.5 regional heavy truck tyre was measured in a climate wind tunnel at a wide range of ambient temperatures. Fig. 23 shows the transient rolling resistance at different ambient temperatures (+25 and -15 °C) and the averaged rolling resistance. Averaged rolling resistance (C_{rr_AVG}, Eq. (23)) describes the rolling resistance that a vehicle has experienced over a certain drive time $\left(t_{drive\_time}\right)$. The rolling resistance increases when the ambient temperature decreases, as shown in Fig. 23. Even though the highest peak of the transient rolling resistance lasts only a short time, it has a significant effect on the average rolling resistance experienced by the vehicle. Consequently, these transient effects should not be neglected, as is commonly the case.

$$C_{rr\_AVG}(t) = \frac{1}{t_{drive\_time}} \int_{t=0}^{t_{drive\_time}} C_{rr}(t)dt. \tag{23}$$

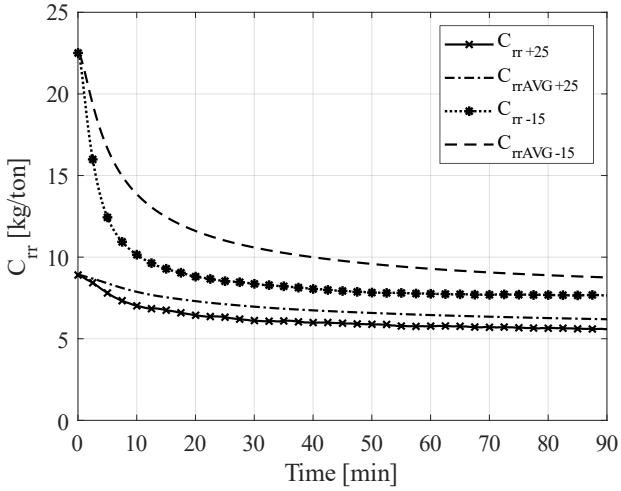

Fig. 23. Transient rolling resistance and averaged rolling resistance plotted over time at +25 and -15 °C. C_{rrAVG} describes the average rolling resistance over certain drive time.

Additionally, the temperature of the truck tyre was measured at the tyre shoulder and apex. The apex measurements reach lower temperatures (Fig. 24 a) and warm up substantially slower (Fig. 24 b) than the measurements at the tyre shoulder. The positioning of the temperature sensors has a significant effect on the quality of temperature measurements as an indicator for rolling resistance. Shoulder temperature is a more suitable indicator for the change of rolling resistance (Fig. 25), whereas apex measurements show consistent rolling resistance values only after a long warm-up. For further information regarding temperature dependency of rolling resistance, see **Paper B**.

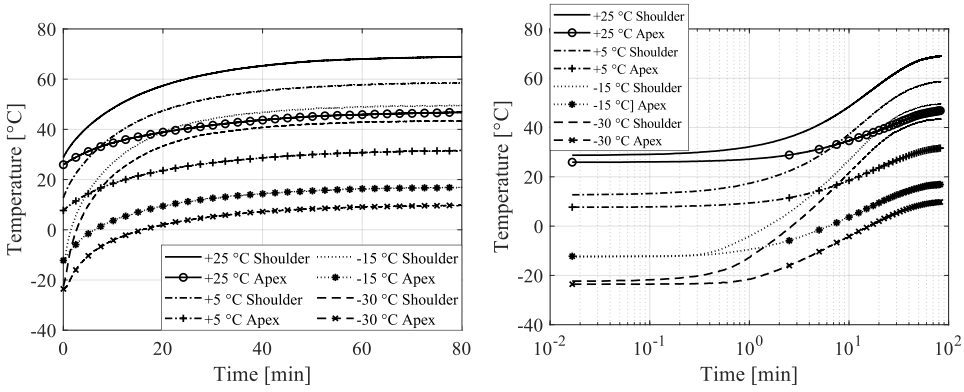

*Fig. 24. Tyre temperature plotted over time at different ambient temperatures from two different measurement positions: tyre shoulder and apex using (left) linear and (right) logarithmic scale (**Paper B**).*

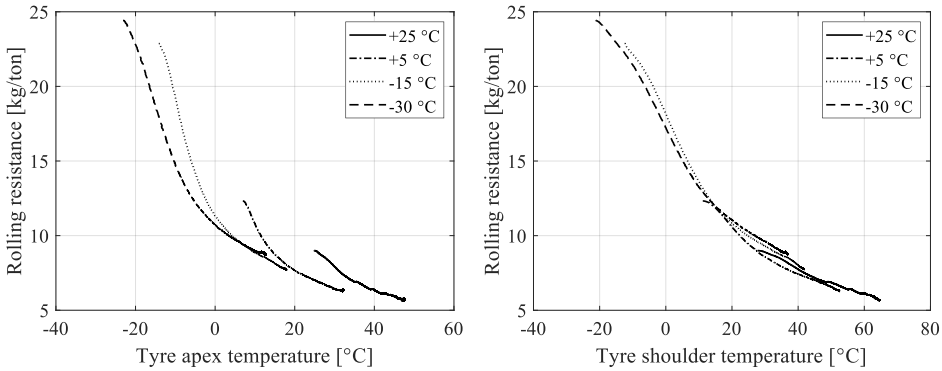

*Fig. 25. The effect of tyre temperature on rolling resistance plotted using temperature measurement from the tyre (left) apex and (right) shoulder (**Paper B**).*

To understand the importance of the change in rolling resistance for future battery-electric trucks (BET), simple calculations were conducted to analyse how great an effect the ambient temperature has on the long haulage BET driving range when air density and rolling resistance are varied with ambient temperature. Fig. 26 shows the difference in air density at different ambient temperatures, where relative air humidity has a negligible effect on air density at a temperature range between -30 to +25 °C. The calculations consider constant velocity, and the averaged rolling resistance was used after driving 155 minutes at different ambient temperatures. The change in driving range is depicted in Fig. 27. The range decreases by approximately 34 % at -30 °C compared to the range at a temperature of +25 °C. For more results, see **Paper B**.

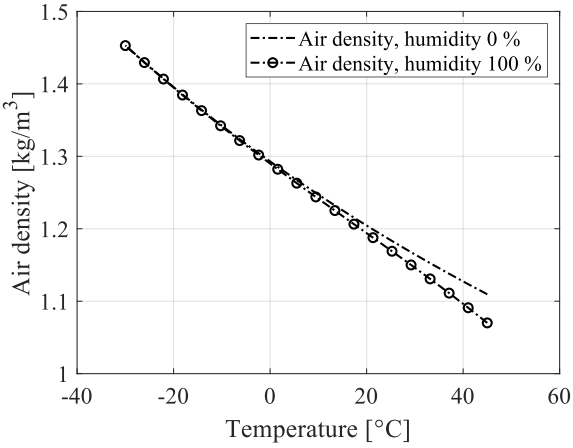

*Fig. 26. The influence of temperature on air density having 0 % and 100 % relative air humidity (**Paper B**).*

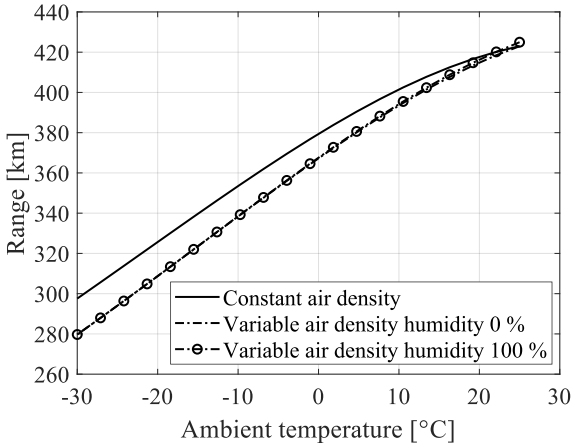

*Fig. 27. The influence of ambient temperature, air density and air humidity on a battery-electric truck range (**Paper B**).*

9 Summary of appended papers

Paper A - Constitutive model suitable for truck tyre rolling resistance simulations
J. Hyttinen, R. Österlöf, L. Drugge and J. Jerrelind
Proceedings of the Institution of Mechanical Engineers, Part D: Journal of Automobile Engineering (December 2021). DOI: 10.1177/09544070221074108

Tyre rubber dissipates mechanical work into heat, which is why the modelling of dissipation and stiffness of tyre rubber is essential for rolling resistance simulations. There have been many attempts to capture tyre rubber mechanical behaviour in rolling resistance simulations. Rolling resistance is most commonly simulated using linear viscoelastic models. Nonlinear viscoelastic models in a parallel rheological model (PRF) have been incorporated recently, but parametrising them is difficult. Additionally, sensitivity studies are problematic when the different parameters are unclear.

This article was the first step in this research to obtain dynamic rubber data and to utilise a hyperviscoplastic finite element rubber model suitable for capturing the Fletcher-Gent effect. Additionally, a parametrisation technique was developed. This method simplifies the parametrisation so that the parameters can be obtained even with manual iterations. The technique provides six reduced parameters that distribute all the other constitutive parameters. The number of these reduced parameters does not increase if more plastic or viscoelastic networks are added. Separate viscous and plastic networks make it easier to tune the amplitude or frequency dependency of the storage and loss modulus. The model is implemented in MATLAB, which allows quick parameter iterations. To highlight the simplicity of the method, the parametrisation against the test data was done using only manual iterations. This is generally not possible for such a complex material model with a large number of material parameters.

The test specimens were extracted from a 385/55 R22.5 long haulage heavy truck tyre and dynamic mechanical analysis was conducted. With the proposed method, a wide range of strain amplitudes and frequencies can be covered, showing good agreement with measurement data. This model and parametrisation technique should be suitable for analysing rolling resistance, as well as simulating other rubber components.

Paper B - Effect of ambient and truck tyre temperature on rolling resistance
J. Hyttinen, M. Ussner, R. Österlöf, J. Jerrelind and L. Drugge
Accepted for publication in the International Journal of Automotive Technology (March 2022).

Rubber has a temperature dependency for its dissipation and stiffness properties. Nevertheless, there is little data on rolling resistance at various operating conditions. Therefore, the rolling resistance of a 315/70 R22.5 regional heavy truck tyre was measured in a wide range of ambient temperatures (-30 °C to +25 °C) in a climate wind tunnel to quantify the importance of temperature on rolling resistance. Additionally, the effect of water cooling on rolling resistance was examined by spraying water on the tyre during the measurement process.

During the tests, two tyre temperatures were measured: tyre shoulder and apex. Tyre shoulder temperature showed to be a good indicator for rolling resistance whereas apex temperature warmed up considerably slower, being a poorer indicator for rolling resistance. The measurements showed that the stabilised rolling resistance increased more than 60 % at at temperature of -30 °C compared to the measurement conducted at +25 °C. When spraying water on the tyre, the rolling resistance increased by approximately 15 %.

To show the importance of the change of rolling resistance at different ambient temperatures, range simulations were conducted for a long haulage battery-electric truck at various ambient temperatures. The simulations showed a decrease of range with lower ambient temperature when both rolling resistance and air density were varied. Tyre manufacturers in Europe are required to provide rolling resistance values according to the ISO 28580 testing standard. These rolling resistance values are acquired after a warm-up of three hours, thereby neglecting the transient rolling resistance. For long haulage driving cycles, the averaged rolling resistance gives a more representative value for assessing energy consumption than the stabilised rolling resistance after three hours of warm-up. For urban and regional driving, the ISO measurement method is expected to differ even more from the actual average rolling resistance experienced by the vehicle.

Paper C - Simulation of a truck tyre using a viscoplastic constitutive rubber model
J. Hyttinen, R. Österlöf, L. Drugge and J. Jerrelind
Presented at IAVSD2021, 27th Symposium on Dynamics of Vehicles on Roads and Tracks, Aug 17-19, St Petersburg, Russia (2021).

A typical tyre design is a compromise between various properties, such as load-carrying capacity, road loads, driving comfort, energy dissipation, and handling. These tyre properties are difficult to improve simultaneously because of opposing requirements. As an example, it might be beneficial from a rolling resistance point of view to have a small contact area, whereas for road maintenance aspects, the loads should be distributed over as large an area as possible. Therefore, to reduce rolling resistance or to balance between conflicting properties, a tyre model should be suitable for several types of tyre analyses.

To gain confidence in the viscoplastic modelling framework introduced in **Paper A**, a tyre model was created in MSC Marc 2021 commercial finite element software. Footprint, vertical stiffness, steady-state rolling, and longitudinal force generation simulations were conducted. The simulations showed that the viscoplastic modelling technique is suitable for different simulations. The model can capture uneven contact pressure in steady state rolling, which causes a large part of the rolling resistance. This is promising for future rolling resistance simulations.

The benefit of the modelling technique is that the material model captures the Fletcher-Gent effect. The viscoplastic modelling technique has the drawback that the frequency stiffening is constant throughout the strain range. At the same time, this is beneficial for model tuning when the whole range is changed at the same time, while still being an adequate approximation of the Fletcher-Gent effect in a finite strain range.

10 Concluding remarks

This thesis aimed to lay out the groundwork for future finite element rolling resistance simulations and quantifying parameters affecting rolling resistance. The main contributions are:

- The proposed material model and parametrisation technique can model the strain amplitude-dependent storage modulus and loss modulus (Fletcher-Gent effect) in a wide range of frequencies and amplitudes **(Paper A)**.
- The developed parametrisation technique enables possibilities for quick design iterations by reducing the tuneable parameters to six. These reduced parameters are not dependent on the amount of plastic or viscoelastic networks **(Paper A)**.
- Separate viscous and plastic networks simplify parameter studies **(Paper A)**.
- The hyperviscoplastic constitutive modelling technique is suitable for different tyre simulations, such as vertical stiffness, longitudinal force generation and footprint analyses **(Paper C)**.
- The modelling technique captures uneven contact pressure in steady-state rolling, which indicates that it could be used in rolling resistance studies **(Paper C)**.
- Ambient temperature significantly affects rolling resistance. Lower ambient temperature results in an increase of rolling resistance due to increased energy dissipation in the tyre rubber **(Paper B)**.
- The positioning of the temperature sensors inside the tyre is important. Thermocouples inside the tyre shoulder is a good indicator for rolling resistance, while apex temperature measurements are less meaningful for indicating rolling resistance **(Paper B)**.
- Spraying water on tyres increases rolling resistance considerably by lowering the tyre temperature **(Paper B)**.
- The driving range of battery-electric trucks reduces substantially with decreasing ambient temperature **(Paper B)**.

11 Future work

Suggestions for future work are illustrated in Fig. 28. Based on the findings during this work, the following points could be examined further. To better understand if the modelling technique is suitable for analysing rolling resistance, further simulations should be conducted. The constitutive model could be improved by adding temperature dependency for the viscoelasticity and plasticity, as well as modelling the Mullins effect. There are two approaches for including temperature in finite element simulations. Either the rubber parameters should be mapped for different temperatures, or a thermomechanical coupling should be implemented directly to the constitutive model.

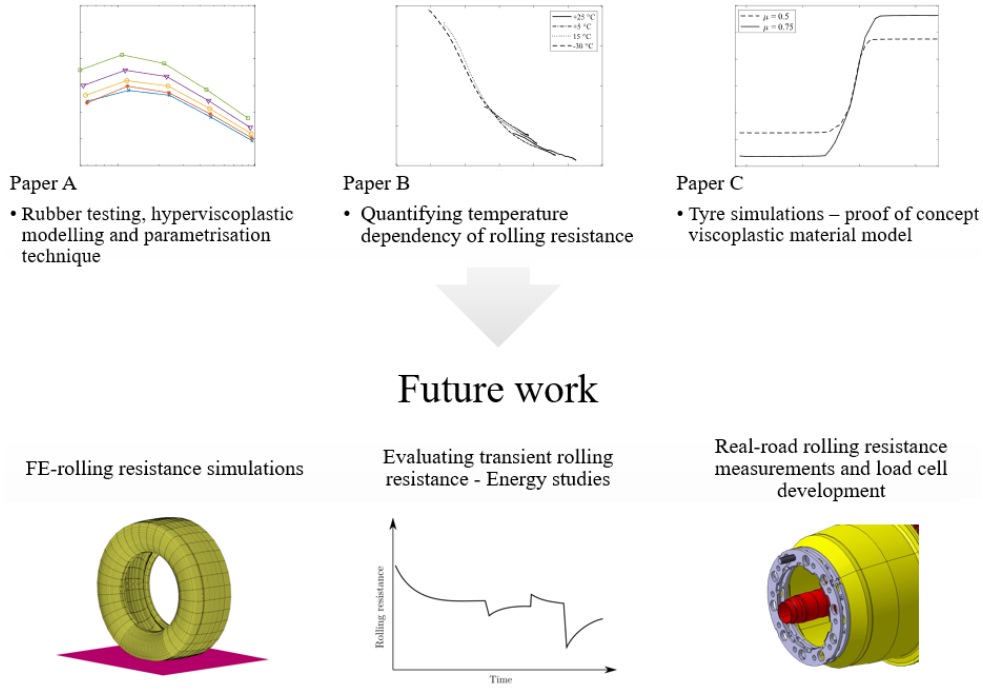

Fig. 28. Suggestions for future work.

Tyre temperature is an area that should be explored in greater depth in the future. There is a strong possibility that a wheelhouse or a rim design that limits heat conduction, convection or radiation away from the tyre could have a reducing effect on rolling resistance. To estimate the remaining range during truck operation, a simple transient rolling resistance modelling approach could be incorporated that takes into account ambient or tyre temperature. Experimental studies on the temperature dependency of rolling resistance could also be performed on real road conditions to gain more confidence in the drum measurements conducted in **Paper B**.

Further on, to develop a quantitative understanding of vehicle-road interaction, other aspects such as tyre pressure, axle loads and lateral forces could be studied using experimental and computational methods. Estimations of transient rolling resistance could even be performed using supervised or unsupervised machine learning methods.

References

[1] "Reducing CO_2 emissions from heavy-duty vehicles," 2019. https://ec.europa.eu/clima/eu-action/transport-emissions/road-transport-reducing-co2-emissions-vehicles/reducing-co2-emissions-heavy-duty-vehicles_en (accessed Feb. 09, 2022).

[2] Y. Nakajima, *Advanced Tire Mechanics*. Springer Singapore, 2019.

[3] J. Hyttinen, R. Österlöf, J. Jerrelind, and L. Drugge, "Development of a vehicle-road interaction analysis framework for truck tyres," REV2021.

[4] M. S. Evans, *Tyre Compounding for Improved Performance, Volume 12. Smithers*, 2001.

[5] B. Rodgers, *Tire engineering: An introduction*, no. 1. CRC Press, 2020.

[6] H. S. Aldhufairi and O. A. Olatunbosun, "Developments in tyre design for lower rolling resistance: A state of the art review," *Proc. Inst. Mech. Eng. Part D J. Automob. Eng.*, vol. 232, no. 14, pp. 1865–1882, 2018, doi: 10.1177/0954407017727195.

[7] D. J. Schuring, "Rolling Loss of Pneumatic Tires.," *Rubber Chemistry and Technology*, vol. 53, no. 3. pp. 600–727, 1980, doi: 10.5254/1.3535054.

[8] J. Bergstrom, *Mechanics of solid polymers : theory and computational modeling*. Elsevier, 2015.

[9] J. Diani, B. Fayolle, and P. Gilormini, "A review on the Mullins effect," *Eur. Polym. J.*, vol. 45, no. 3, pp. 601–612, 2009, [Online]. Available: https://doi.org/10.1016/j.eurpolymj.2008.11.017.

[10] G. Holzapfel, *Nonlinear solid mechanics: a continuum approach for engineering*. Wiley, 2000.

[11] M. J. García Tárrago, L. Kari, J. Vinolas, and N. Gil-Negrete, "Frequency and amplitude dependence of the axial and radial stiffness of carbon-black filled rubber bushings," *Polym. Test.*, vol. 26, no. 5, pp. 629–638, 2007, doi: 10.1016/j.polymertesting.2007.03.011.

[12] A. N. Gent, *Engineering with Rubber 3e: How to Design Rubber Components*. HANSER PUBN, 2012.

[13] I. M. Ward and J. Sweeney, *Mechanical Properties of Solid Polymers*. Wiley, 2013.

[14] "SS-ISO 9924-3:2009," 2009.

[15] N. Warasitthinon and C. G. Robertson, “Interpretation of the tand peak height for particle-filled rubber and polymer nanocomposites with relevance to tire tread performance balance,” *Rubber Chem. Technol.*, vol. 91, no. 3, pp. 577–594, 2018, doi: 10.5254/rct.18.82608.

[16] “SS-ISO 48-2:2018,” 2018.

[17] E. Duell, A. Kharazi, P. Nagle, P. Elofsson, D. Söderblom, and C. M. Ramden, “Scania’s New CD7 Climatic Wind Tunnel Facility for Heavy Trucks and Buses,” *SAE Int. J. Passeng. Cars - Mech. Syst.*, vol. 9, no. 2, 2016, doi: 10.4271/2016-01-1614.

[18] “ISO 28580:2009,” 2009.

[19] S. K. Clark and R. N. Dodge, “A handbook for the rolling resistance of pneumatic tires,” Ann-Arbor, 1979. [Online]. Available: http://deepblue.lib.umich.edu/bitstream/handle/2027.42/4274/bac0913.0001.001.pdf.

[20] C. Daesa and S. Rodkwan, “Prediction of rolling resistance coefficient of retreaded truck tyres through numerical simulation,” *Maejo Int. J. Sci. Technol.*, vol. 12, no. 2, pp. 152–166, 2018.

[21] R. Ali, R. Dhillon, M. El-Gindy, F. Öijer, I. Johanson, and M. Trivedi, “Prediction of rolling resistance and steering characteristics using finite element analysis truck tyre model,” *Int. J. Veh. Syst. Model. Test.*, vol. 8, no. 2, pp. 179–201, 2013, doi: 10.1504/IJVSMT.2013.054475.

[22] B. Mashadi, S. Ebrahimi-Nejad, and M. Abbaspour, “A rolling resistance estimate using nonlinear finite element numerical analysis of a full three-dimensional tyre model,” *Proc. Inst. Mech. Eng. Part D J. Automob. Eng.*, vol. 233, no. 1, pp. 147–160, 2019, doi: 10.1177/0954407018802733.

[23] J. A. Hernandez, I. L. Al-Qadi, and H. Ozer, “Baseline rolling resistance for tires’ on-road fuel efficiency using finite element modeling,” *Int. J. Pavement Eng.*, vol. 18, no. 5, pp. 424–432, 2017, doi: 10.1080/10298436.2015.1095298.

[24] T. Dalrymple, J. Hurtado, I. Lapczyk, and H. Ahmadi, “Parallel rheological framework to model the amplitude dependence of the dynamic stiffness in carbon-black filled rubber,” in *Constitutive Models for Rubbers IX*, CRC Press , 2015, pp. 189–195.

[25] M. Rafei, M. H. R. Ghoreishy, and G. Naderi, “Computer simulation of tire rolling resistance using finite element method: Effect of linear and nonlinear viscoelastic models,” *Proc. Inst. Mech. Eng. Part D J. Automob. Eng.*, vol. 233, no. 11, pp. 2746–2760, 2019, doi: 10.1177/0954407018804117.

[26] N. Gil-Negrete, J. Vinolas, and L. Kari, “A Nonlinear rubber material model combining fractional order viscoelasticity and amplitude dependent effects,” *J. Appl. Mech. Trans. ASME*, vol. 76, no. 1, pp. 1–9, 2009, doi: 10.1115/1.2999454.

[27] Abaqus, “Abaqus docs - Parallel rheological framework.” https://abaqus-docs.mit.edu/2017/English/SIMACAEMATRefMap/simamat-c-nonlinvisco.htm (accessed Mar. 11, 2022).

[28] P.-E. Austrell and A. K. Olsson, “Modelling procedures and properties of rubber in rolling contact,” *Polym. Test.*, vol. 32, no. 2, pp. 306–312, Apr. 2013.

[29] E. M. Arruda and M. C. Boyce, “A three-dimensional constitutive model for the large stretch behavior of rubber elastic materials,” *J. Mech. Phys. Solids*, vol. 41, no. 2, pp. 389–412, 1993, doi: 10.1016/0022-5096(93)90013-6.

[30] M. Mooney, “A Theory of Large Elastic Deformation,” *J. Appl. Phys.*, vol. 11, no. 9, pp. 582–592, 1940, [Online]. Available: https://doi.org/10.1063/1.1712836.

[31] N. H. Kim, *Introduction to nonlinear finite element analysis*. Springer New York, 2015.

[32] L. Anand, “Moderate deformations in extension-torsion of incompressible isotropic elastic materials,” *J. Mech. Phys. Solids*, vol. 34, no. 3, pp. 293–304, Jan. 1986.

[33] R. Österlöf, H. Wentzel, and L. Kari, “A finite strain viscoplastic constitutive model for rubber with reinforcing fillers,” *Int. J. Plast.*, vol. 87, pp. 1–14, Dec. 2016.

[34] J. Ejsmont, S. Taryma, G. Ronowski, and B. Swieczko-Zurek, “Influence of temperature on the tyre rolling resistance,” *Int. J. Automot. Technol.*, vol. 19, no. 1, pp. 45–54, Feb. 2018, [Online]. Available: https://doi.org/10.1007/s12239-018-0005-4.

[35] M. L. Janssen and G. L. Hall, “Effect of ambient temperature on radial tire rolling resistance,” *SAE Tech. Pap.*, vol. 89, no. 1980, pp. 576–580, 1980, doi: 10.4271/800090.

[36] M. Greiner, H. J. Unrau, and F. Gauterin, “A model for prediction of the transient rolling resistance of tyres based on inner-liner temperatures,” *Veh. Syst. Dyn.*, vol. 56, no. 1, pp. 78–94, 2018, doi: 10.1080/00423114.2017.1343955.

[37] W. V. Mars and J. R. Luchini, “Analytical model for the transient rolling resistance behavior of tires,” *Tire Sci. Technol.*, vol. 27, no. 3, pp. 161–175, 1999, doi: 10.2346/1.2135982.

[38] J. R. Luchini and J. A. Popio, “Modeling transient rolling resistance of tires,” *Tire Sci. Technol.*, vol. 35, no. 2, pp. 118–140, 2007, doi: 10.2346/1.2737562.

[39] O. Bode, “FAT-Schriftenreihe 325.” Verband der Automobilindustrie (VDA), Hannover, 2020, [Online]. Available: vda.de/vda/de/aktuelles/publikationen/publication/fat-schriftenreihe-325.

[40] J. Ejsmont, L. Sjögren, B. Świeczko-Żurek, and G. Ronowski, “Influence of Road Wetness on Tire-Pavement Rolling Resistance,” *J. Civ. Eng. Archit.*, vol. 9, no. 11, Nov. 2015.

[41] T. Sandberg, C. Ramdén, and M. Gamberg, “Tire Temperature Measurements for Validation of a New Rolling Resistance Model,” *IFAC Proc. Vol.*, vol. 37, no. 22, pp. 589–594, 2004, doi: 10.1016/s1474-6670(17)30407-x.

Part II
APPENDED
PAPERS A-C